



U·P·O·J

Wei-Ju Tseng, MSE  
Tiao Lin, MD  
Chantal MJ de Bakker  
L. Scott Levin, MD, FACS  
Ling Qin, PhD  
X. Sherry Liu, PhD

University of Pennsylvania,  
Philadelphia, PA, USA

# Changes in the Trabeculae-Vessel Function Unit in Response to Estrogen Deficiency-Induced Bone Loss and Intermittent Parathyroid Hormone-Induced Bone Gain

## Introduction

The bone remodeling process is required to repair damaged bone tissue and more importantly, to regulate calcium and phosphate homeostasis in conjunction with the microvascular network within bone marrow. However, simultaneous visualization of the trabecular and vascular microstructures remains challenging, and thus the precise relationship between blood vessel formation and trabecular remodeling, as well as the impact of this relationship on metabolic bone diseases such as osteoporosis, remains unclear. In our recent study, we observed a trend of positive correlation between blood vessel number and trabecular number in rats. Therefore, we hypothesized that the volume and number of blood vessels are associated with those of trabeculae. We used a well-described bone loss model by inducing estrogen deficiency in ovariectomized (OVX) rats<sup>1</sup> and a bone gain model by administering intermittent parathyroid hormone (PTH) in intact rats.<sup>2</sup> Together with vehicle-treated intact rats, we aimed to generate samples with a wide spectrum of trabecular bone and vessel densities. Critical to the advancement of bone vasculature research is the development of a 3-dimensional (3D) simultaneous visualization of the trabecular and vascular microstructures. In this study, we developed a novel vascular network perfusion technique combining standard  $\mu$ CT and image processing techniques to simultaneously visualize and quantify the 3D trabecular and vascular microstructures in the rat tibia. The objective of this study was to investigate the changes in the trabeculae-vessel function unit in response to estrogen deficiency-induced bone loss and intermittent PTH-induced bone gain models.

## Methods

### Study Design

Six intact and three ovariectomized female Sprague-Dawley rats (90 days old) were purchased and housed at the animal facility

for 60 days prior to the experiment (IACUC approved). The six intact rats were divided into saline-treated (VEH) and PTH-treated groups at 150 days old. Both VEH (saline) and PTH (PTH 1-34, 60 $\mu$ g/kg/day, Bachem) groups received subcutaneous injections 5 days/week for 2 weeks.

### In Vivo $\mu$ CT Scans

At the end of treatment, the left tibiae from rats in all three groups were scanned using the vivaCT 40 scanner (Scanco Medical AG) while the rats were under anesthesia. A 10-mm region located distal to the proximal growth plate was scanned for each tibia at 10.5 $\mu$ m resolution.

### Perfusion

Following *in vivo* scans, a catheter was inserted into the abdominal aorta, and an incision was made in the right atrium. A three-step perfusion protocol was used. Using a perfusion pump, 50 mL of heparin sodium (30 units/mL) followed by 100 mL of 0.9% saline were infused at 4.4 mL/min through the rat. Next, using a syringe pump, 4.5 mL of freshly mixed Microfil (MV122, FlowTech) was injected into the aorta at 1 mL/min. Once the mixture reached the common iliac arteries, the flow rate was decreased to 0.3 mL/min. The perfusion mixture was prepared by diluting a silicone rubber injection compound 4:1 with medium-viscosity diluent and mixing the result with 4.5% curing agent. The perfused animals were stored at 4 °C for 24 hours. Tibiae were harvested and fixed in 4% formalin.

### Post-Perfusion Scans

A 10mm-thick region located distal to the proximal growth plate was scanned at a 6 $\mu$ m resolution using the  $\mu$ CT 35 scanner (Scanco Medical AG).

### Image Registration

A registration procedure at 10.5  $\mu$ m resolution was employed using a landmark-initialized, mutual-information-based registration kit (ITK,

NLM). Post-perfusion scans (containing both bone and blood vessel) were registered to pre-perfusion scans (containing bone only), which allowed the same region of interest to be analyzed in both scans. A custom program was used to separate the vessels from the registered scans. Trabecular and vasculature structures were quantified in a 6 mm region distal to the growth plate. Trabecular and vessel volume fraction (Tb.BV/TV and Ves.V/TV), trabecular and vessel number (Tb.N and Ves.N), trabecular and vessel thickness (Tb.Th and Ves.Th), and trabecular and vessel spacing (Tb.Sp and Ves.Sp) of each group were measured.

### Statistics

Comparisons between VEH and PTH groups and between VEH and OVX groups were made using 2-tailed student's *t*-tests with  $p < 0.05$  indicating significance and  $p < 0.1$  indicating trends.

## Results

### OVX vs. VEH

As expected, trabecular bone in the OVX group had 69% lower Tb.BV/TV ( $p < 0.05$ ), 75% lower Tb.N ( $p < 0.05$ ), 400% higher Tb.Sp ( $p < 0.05$ ), and trends toward a lower Tb.Th (11%,  $p < 0.1$ ) compared to that of the VEH group (Figure 1). Vessels in the OVX group were 82% thicker than those in the VEH group ( $p < 0.05$ , Figure 2). There was no measurable difference

in Ves.BV/TV, Ves.N or Ves.Sp between the VEH and OVX groups.

### PTH vs. VEH

There was no significant difference in Tb.BV/TV, Tb.N or Tb.Sp between PTH and VEH groups, with a trend of increase in Tb.Th in the PTH group (8%,  $p < 0.1$ , Figure 1F). To confirm PTH's anabolic effect on bone, trabecular bone measurements after PTH treatment were also compared with those at the beginning of treatment measured by *in vivo*  $\mu$ CT. Longitudinal comparisons confirmed that there was a 22% increase in Tb.BV/TV and 18% in Tb.Th ( $p < 0.05$ ) due to a 2-week PTH treatment. Moreover, compared to the VEH group, the PTH group had trends toward higher Ves.V/TV (53%,  $p < 0.1$ , Figure 2D), Ves.N (38%,  $p < 0.1$ , Figure 2E), and 34% lower Ves.Sp ( $p < 0.1$ , Figure 2G). There was no significant difference in Ves.Th between PTH and VEH groups.

## Discussion

In this study we developed an imaging framework to simultaneously visualize 3D trabecular microstructure and microvasculature inside the tibiae of both OVX rats and PTH-treated rats (Figures 1 and 2). Following an 8-week development of osteoporosis, OVX rats showed systemic deteriorations in trabecular bone microstructure and a significant increase in vessel thickness compared to the VEH rats. This result did not support our hypothesis, suggesting that estrogen-induced

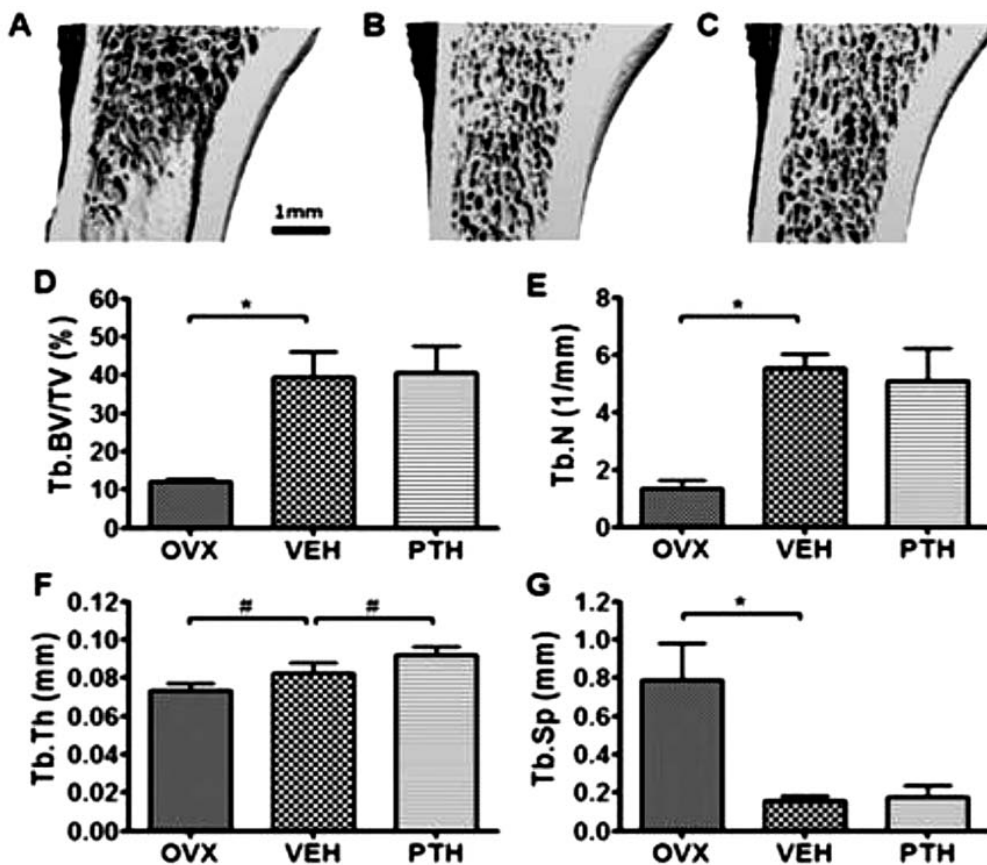


**Figure 1.** 3D representative bone images of (A) OVX, (B) VEH, (C) PTH groups; 3D microstructure analysis of trabecular bone: (D) Trabecular Volume Fraction (E) Trabecular Number, (F) Trabecular Thickness, (G) Trabecular Spacing. Mean  $\pm$  SD, \*:  $p < 0.05$ , #:  $p \leq 0.01$ .

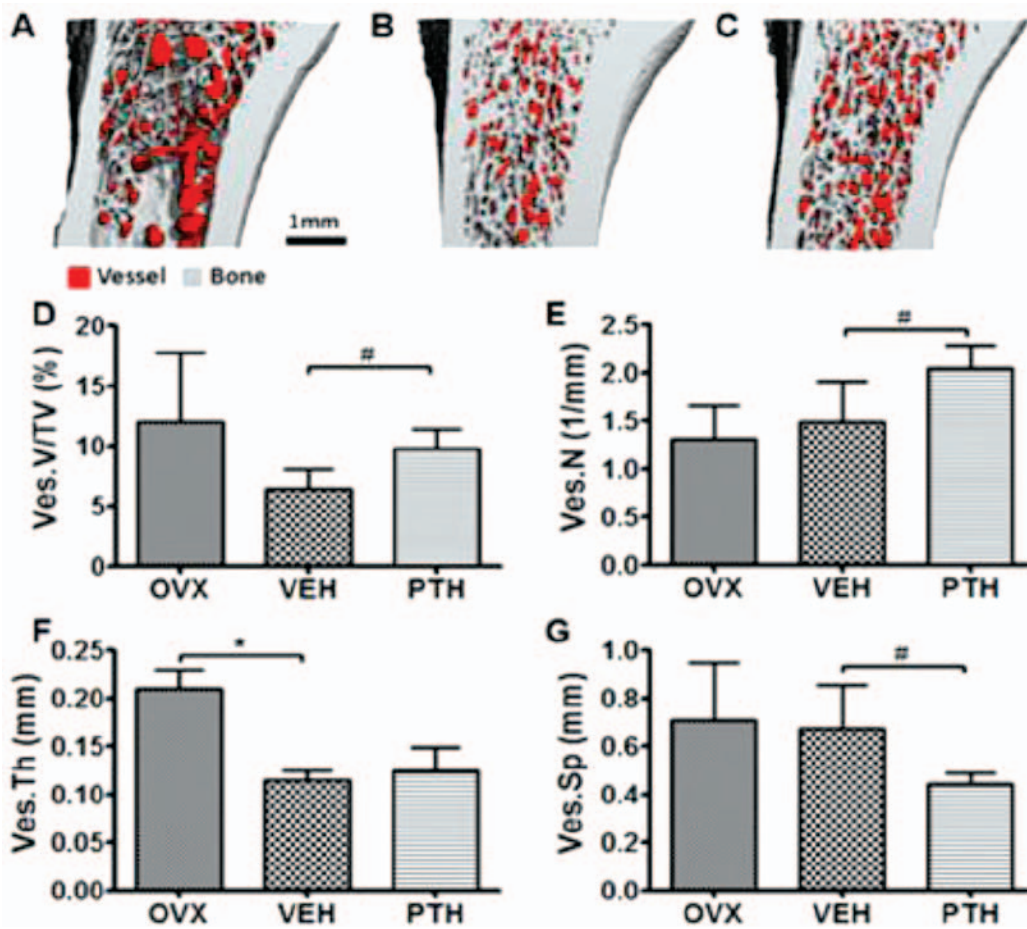


**Figure 2.** 3D representative bone and vessel images of (A) OVX, (B) VEH, (C) PTH groups; 3D microstructure analysis of vasculature: (D) Vessel Volume Fraction, (E) Vessel Number, (F) Vessel Thickness, (G) Vessel Spacing, Mean  $\pm$  SD, \*:  $p < 0.05$ , #:  $p \leq 0.01$ .

bone loss is not necessarily associated with reduced blood vessels. Compared to VEH-treated rats, PTH-treated rats tended to have greater vessel volume and number and reduced vessel spacing, which is consistent with Kang *et al's* recent report in a murine mandibular model of distraction osteogenesis and angiogenesis following 21 days intermittent PTH treatment.<sup>3</sup> On the other hand, our results were inconsistent with Prisby *et al's* report,<sup>4</sup> which did not find improved angiogenesis after PTH treatment. However, the discrepancy may be due to use of different PTH analogues (1-34 versus 1-84) and rat sex (female versus male). Both PTH treatment and OVX result in accelerated bone remodeling, but with opposite net balance towards formation and resorption, respectively. Interestingly, our results showed increases or trends toward increase in blood vessels in both PTH and OVX rats, suggesting a possible association between angiogenesis and bone remodeling rate. More studies need to be done to test this hypothesis.

## Significance

This study establishes a novel technique that simultaneously visualizes the 3D microstructures of bone and microvasculature

using standard  $\mu$ CT in both an OVX rat model and an intermittent PTH-treated rat model, resulting in an improved understanding of the effects of OVX and intermittent PTH on the bone-blood vessel function unit.

## Acknowledgments

This study was partially supported by Penn Center for Musculoskeletal Disorders (NIH/NIAMS P30 AR050950). We'd like to thank A. Altman, PhD and K. Britton for their technical assistance.

## References

1. Kalu DN. The ovariectomized rat model of postmenopausal bone loss. *Bone Miner.* 15, 175–191 (1991).
2. Qin L, Raggatt LJ, Partridge NC. Parathyroid hormone: a double-edged sword for bone metabolism. *Trends Endocrinol. Metab. TEM* 15, 60–65 (2004).
3. Kang SY, et al. Parathyroid hormone reverses radiation induced hypovascularity in a murine model of distraction osteogenesis. *Bone* 56, 9–15 (2013).
4. Prisby R, et al. Intermittent PTH(1-84) is osteoanabolic but not osteoangiogenic and relocates bone marrow blood vessels closer to bone-forming sites. *J. Bone Miner. Res.* 26, 2583–2596 (2011).